Liquefaction Assessment of Thin Sand Layers with Partially Drained Condition

M. Okamura[1], F.C. Nelson[2]

ABSTRACT

More than 2000 river levees were damaged by the 2011 Off the Pacific Coast of Tohoku Earthquake and liquefaction of relatively thin soils layers in levees is considered to be the fundamental mechanism of about 80% the damaged levees. It is revealed that the liquefaction assessment method provides the factor of safety against liquefaction, F_L, for relatively thin saturated layers in levees excessively on the safe side. A possible reason for this is drainage of generated excess pore pressures during the earthquake shaking. In this study, an attempt was made to improve the liquefaction evaluation method by taking the drainage effects into account. A series of dynamic centrifuge test was carried out on the models of a 1 m deep prototype loose sand deposit with permeability coefficient being varied in a wide range. It was found that the input base accelerations needed to make the soil liquefy increase with increasing permeability and thus amount of drained water during shaking. This increase in the apparent liquefaction resistance is expressed as a function of volumetric strain due to the drainage until soil liquefies and can be taken into account in the calculation of F_L.

Introduction

River levees have repeatedly been damaged by earthquakes and occurrence of crest settlement larger than half of the levee height is not unusual when foundation soils liquefy (Matsuo, 1999). Levees resting on non-liquefiable soil, however, were considered to have rarely experienced severe damage. Recorded crest settlement due to the deformation of soft foundation clay was, at the largest, 15% of the levee height (River Front Center, 1999). In 1993, the Kushiro-oki earthquake hit the northern part of Japan and the Kushiro river levees were severely damaged. The incident attracted attention of engineers since damaged levees were underlain by a non-liquefiable peat deposit. It was presumed that the surface of the highly compressible and less permeable peat deposits below the levees had subsided in a concave shape and a saturated zone formed in the levees liquefied (Sasaki et al., 1995). More recently, more than 2000 river levees were damaged by the 2011 off the Pacific Coast of Tohoku Earthquake (River Bureau, Ministry of Land, Infrastructure and Transport, 2011) and a considerable number of levees failed in this mechanism. Figure 1 illustrates a cross section of such a damaged levee, which was originally approximately 9 m high and rested on a thick alluvium clay deposit (Tohoku Regional Development Bureau, MLIT, 2011). The water table in the levee observed 7 weeks after the earthquake with excavated boreholes was more than 2 m above the foundation clay layer (Ac1), indicating that the lower part of the levee (Bs) was saturated. The soils of the levee (Bs) were mostly silty sands with the SPT N-values lower than 5. The levee spread laterally on the rice pad

[1]Professor, Graduate School of Science and Engineering, Ehime University, Japan, okamura@cee.ehime-u.ac.jp
[2] PhD student, Graduate School of Science and Engineering, Ehime University, Japan, fred.tcharles@gmail.com

which remained intact and many cracks and fissures appeared on the slope were partly filled with boiled sand. All these facts suggest that the levee liquefied. It is interesting to note that neighboring undamaged levees and their foundation soil conditions were quite similar to those of the damaged levees in all aspects with an exception of the water table in the levee being slightly lower (Tohoku Regional Development Bureau, MLIT, 2011). This alludes to the effects of drainage of pore water from saturated soil layers on the occurrence of liquefaction and severity of damage.

In order to assess liquefaction potential of levees, the validity of the evaluation method of in-situ liquefaction susceptibility is important. Okamura and Hayashi (2014) picked out 18 severely damaged levees where liquefaction of soils inside the levees are considered as a main cause of damage. Another 12 undamaged levees in the neighborhood of those damaged levees were also selected. They found that the safety factors against liquefaction, F_L, of all 30 levees calculated with the method of the Japan Road Association (JRA, 2012) were lower than unity for both damaged and undamaged levees. The factor of safety assessed the liquefaction potential of thin saturated sand layers in the levees excessively on the safe side. A possible explanation to this fact may be that the soils in the saturated zones of those levees did not liquefy because generated excess pore pressures dissipated swiftly during earthquake owing to shorter drainage distances and higher permeability of soils. In this study the drainage effects on the liquefaction potential of thin sand layers is studied through a series of centrifuge tests.
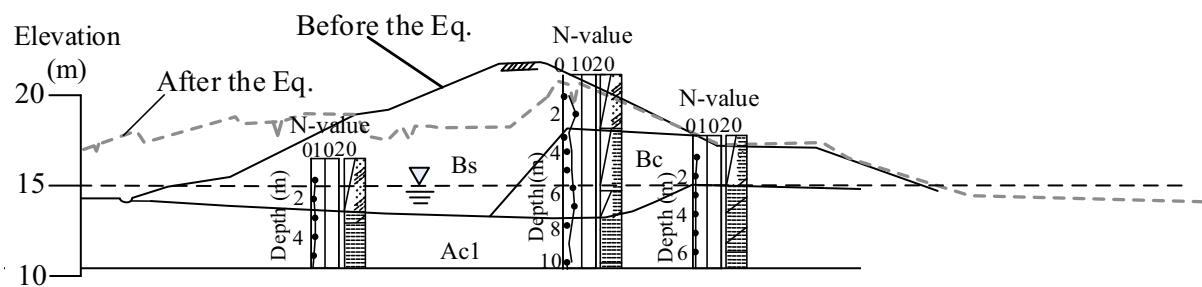

Figure 1. Damaged levee of the Naruse river with SPT N values obtained after the EQ.

Centrifuge Tests

In this section, a series of dynamic centrifuge tests performed in this study is described, which aimed to investigate how the drainage during shaking affects pore pressure responses and accelerations needed to liquefy relatively thin sand layers.

Model preparation and test conditions

Two types of models shown in Figure 2 were tested in a centrifuge at 25g. Model 1 consisted of a 1 m deep uniform sand deposit with the ground water table at the surface, while the model 2 was a saturated uniform sand layer with of the same density and thickness as model 1 and with an overlying 1 m deep unsaturated sand layer.
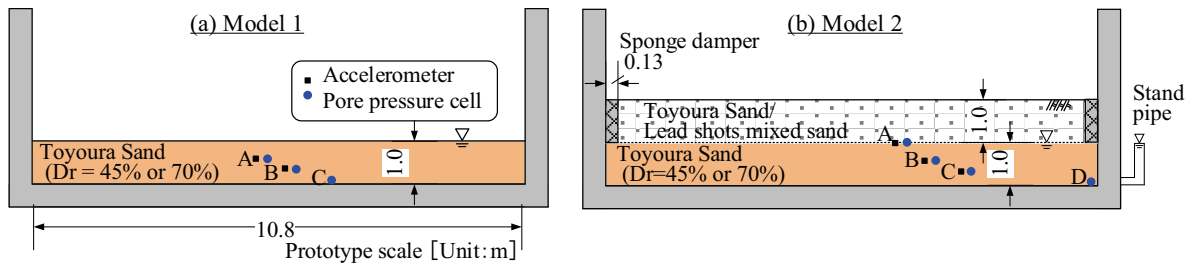
Figure 2. Centrifuge models.

The soil used to build the models was Toyoura sand of which index physical properties are ρ_s= 2.64, e_{max} = 0.973 and e_{min} = 0.609. Dry Toyoura sand was ari pluviated to a relative density of 45% or 70% in a rigid container. For model 2, 5 mm thick sponges were glued on the side walls to allow the upper unsaturated sand layer to displace horizontally during shaking. The same sand or the sand mixed with lead shots was used to build the unsaturated layer in the model 2. The lead shots were employed to increase the overburden pressure without changing geometry of the model. The existence of the overlying unsaturated layer may affects dissipation of excess pore pressures in the underlying saturated layer in two ways; (1) increase in the overburden pressure, and then enhanced hydraulic gradient in the saturated layer, accelerates the dissipation of pore pressures, and (2) obstruct dissipation due to lower permeability. In order to study these effects two type of models with different overburden pressures were prepared in this study.
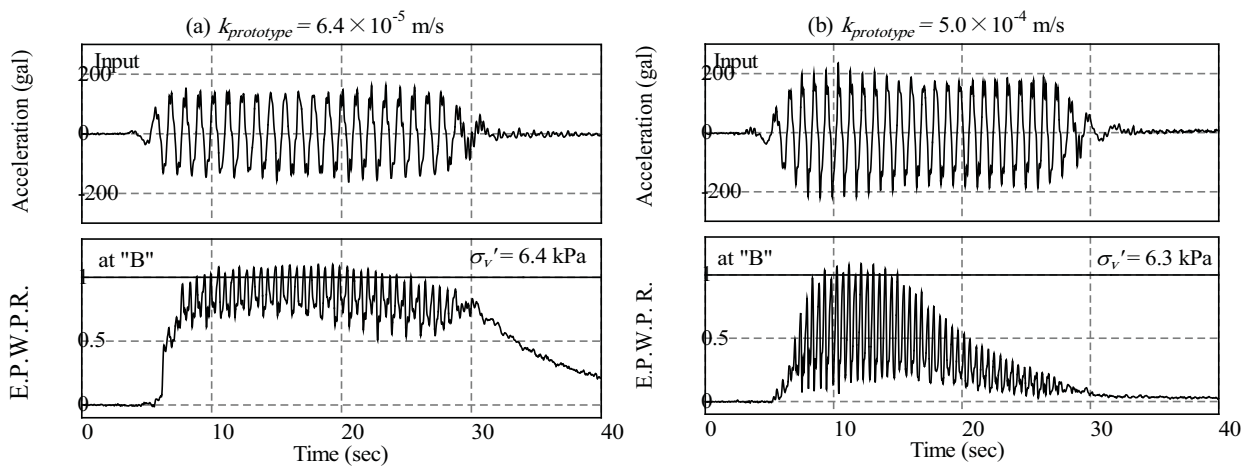

Figure 3. Typical acceleration and excess pore pressure time histories of Model 1 (Dr = 70%).

All the models were fully saturated with water or viscous fluid in a vacuum chamber at a vacuum pressure of -95 kPa with the aid of CO_2 replacement technique to a degree of saturation higher than 99.5%, which was measured with the method developed by Okamura & Inoue (2010). The viscous fluid was a mixture of water and hydroxypropyl methylcellulose. The viscosity of fluid varied from 5cSt to 1000cSt by changing the concentration of the solution. The consequence of using the pore fluid with a viscosity ν times higher than that of water in the centrifuge tests at 25g to model the liquefaction of the water-saturated prototype soil in the field is that the actual

prototype permeability being simulated was $k_{prototype} = k_{model}/\nu*25$. The coefficients of permeability of Toyoura sand k_{model} are 2.5×10^{-4} m/s at Dr = 45% and 1.8×10^{-4} m/s at Dr = 70%. The model was set on the geotechnical centrifuge at Ehime University and the centrifugal acceleration was gradually increased to 25g. For model 2, the pore fluid was drained through a stand pipe until the ground water table stabilized at the proper height. Horizontal base shaking was imparted to the models with the basic shape of acceleration time histories shown in Figure 3. Test conditions are summarized in Table 1.

Table 1 Summary of test conditions and results

Model	Dr (%)	Pore fluid viscosity, ν (cSt)	$k_{prototype}$ (m/s)	σ_v' at mid-depth of saturated layer (kPa)	Input acc. a_{max} (gal)	Number of cycles to liquefy	Model	Dr (%)	Pore fluid viscosity, ν (cSt)	$k_{prototype}$ (m/s)	σ_v' at mid-depth of saturated layer (kPa)	Input acc. a_{max} (gal)	Number of cycles to liquefy
1	45	1	6.3×10^{-3}	4.4	255	3	2	45	10	6.3×10^{-4}	19	249	5
		4	1.6×10^{-3}		199	3			25	2.5×10^{-4}		259	19
		5	1.3×10^{-3}		169	2			10	6.3×10^{-4}	33	504	13
		10	6.3×10^{-4}		152	3			25	2.5×10^{-4}		382	5
		10	6.3×10^{-4}		143	2			120	5.2×10^{-5}		229	8
		24	2.6×10^{-4}		112	2							
		120	5.2×10^{-5}		104	4							
		120	5.2×10^{-5}		73	7							
		280	2.2×10^{-5}		86	19							
		500	1.3×10^{-5}		81	7							
	70	9	5.0×10^{-4}	4.7	205	3		70	9	5.0×10^{-4}	20	455	4
		18	2.5×10^{-4}		198	5			29	1.6×10^{-4}		324	10
		27.5	1.6×10^{-4}		198	11							
		50	9.0×10^{-5}		190	5							
		70	6.4×10^{-5}		140	4							
		220	2.0×10^{-5}		104	15							
		1000	4.5×10^{-6}		105	2							

Results and Discussions

Figure 3 shows typical time histories of input acceleration and excess pore pressure response during shaking observed in tests of model 1 with *Dr* = 70%. The excess pore pressures depend clearly on the permeability, $k_{prototype}$; the model with $k_{prototype} = 6.4\times10^{-5}$ m/s liquefied in a few cycles of shaking with an acceleration amplitude 140 gal, while the model with the higher permeability $k_{prototype} = 5.0\times10^{-4}$ m/s needed a higher acceleration of 205 gal to liquefy and begun to dissipate pore pressure during shaking.

The maximum acceleration amplitudes of the input motions until the soil liquefied are plotted against the prototype permeability for all tests of models 1 and 2 in Figure 4. The number of cycles to reach the liquefaction condition (i.e. excess pore pressure ratio = 1) is indicated in the parentheses. For cases of model 1, the acceleration amplitudes seems to be constant for $k_{prototype}$ lower than 10^{-5} m/s and increases with increasing $k_{prototype}$ for the higher permeability, with the acceleration amplitude being higher for higher relative density.
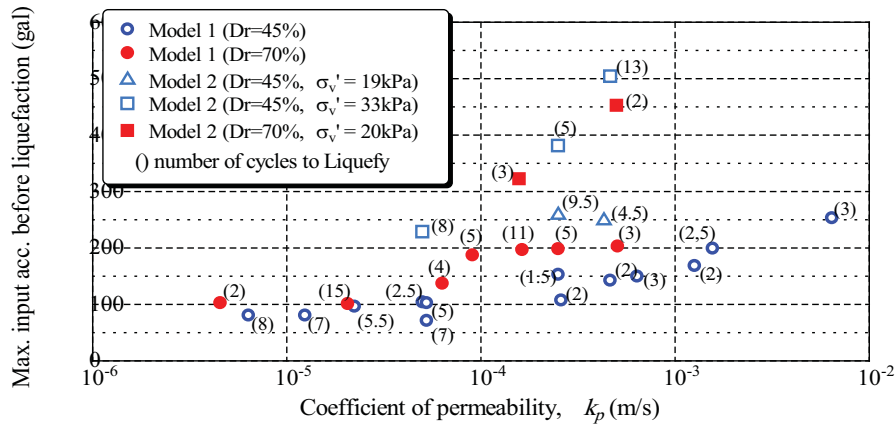
Figure 4. Relationship between acceleration needed to liquefy and permeability of sand.

The accelerations for model 2, in which liquefiable sand layers were overlain by unsaturated layers, are higher than those for model 1 and this is more significant for cases with higher overburden pressure ($\sigma_v' = 33$kPa). Existence of the overlying unsaturated soil layer which decreased the cyclic stress ratio is responsible for this. Factors of safety against liquefaction F_L for each tests were estimated as follows. Because of the different number of cycles to liquefy in each test as indicated in the figure, cyclic stress ratios corresponding to the number of cycles were employed as liquefaction resistance $R_L = CSR_{(N)}(1+2K_0)/3$, where $CSR_{(N)}$ and K_0 denote the cyclic stress ratio at number of cycles N and the coefficient of earth pressure at rest (= 0.5), respectively. Undrained cyclic torsional shear test results on Toyoura sand indicated in Figure 5 (Tanaka et al., 2009) were used for this purpose.

Maximum accelerations a_{max} used to estimate the cyclic stress ratio were the maximum input acceleration before the soils liquefied. The inverse of the factor of safety, that is the apparent liquefaction strength ratio, $1/F_L$, is shown in Figure 6, which is the rate of increase in the shear stress ratio to liquefy the sand due to the drainage effect. $1/F_L$ is approximately unity in the range of $k_{prototype}$ lower than 10^{-5} m/s and increases with increasing $k_{prototype}$ regardless of the relative densities and the overburden pressures.
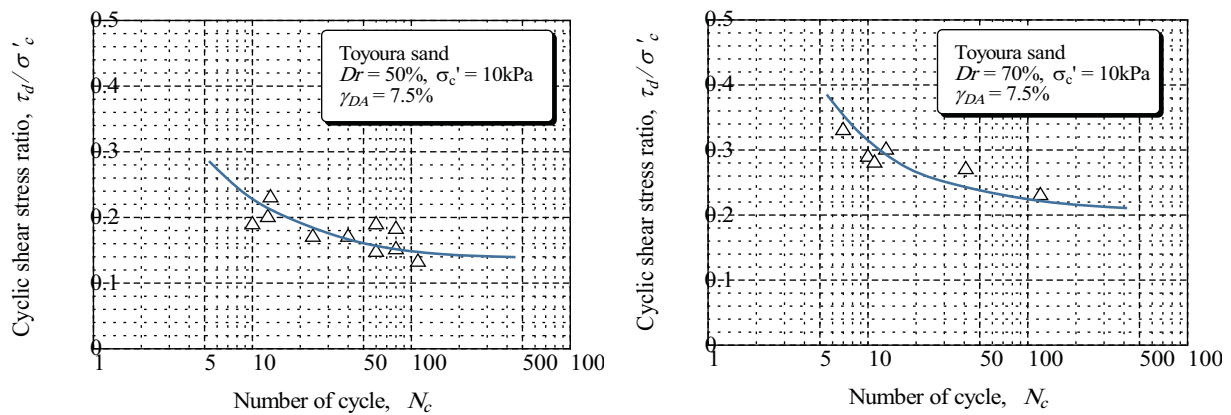
Figure 5. Liquefaction strengths obtained from torsional cyclic shear tests at low confining stress (Tanaka et al., 2009).
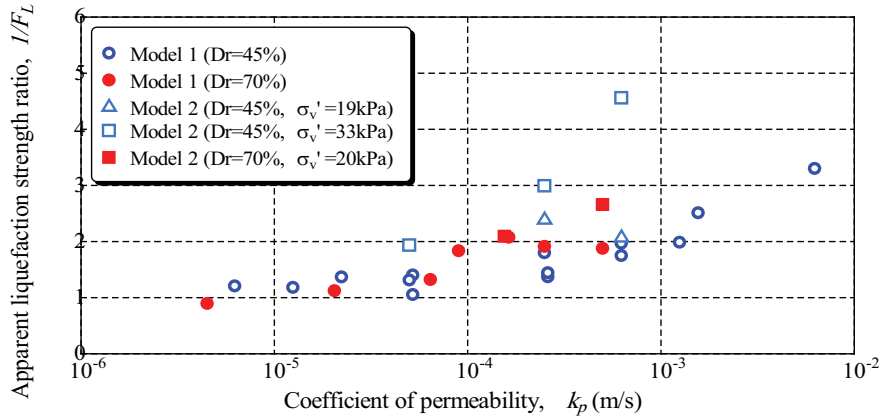

Figure 6. Variation in $1/F_L$ with permeability of sand.

Volumetric Strain due to Drainage

It is common practice to assume the undrained condition to assess a potential for liquefaction, however, the centrifuge test results described above clearly indicates that the undrained condition does not hold true depending on permeability. The apparent liquefaction resistance increased with increasing permeability and thus with amount of drained water from the layer during shaking. Increases in apparent liquefaction resistance have also been observed in studies related to the membrane penetration and imperfect saturation of specimen.

$$\varepsilon_v^* = \frac{\sigma_c'}{p_0 + \sigma_c'}\left(1 - S_r\right)\frac{e}{1+e}$$

S_r : degree of saturation

σ_c' : initial effective confining pressure

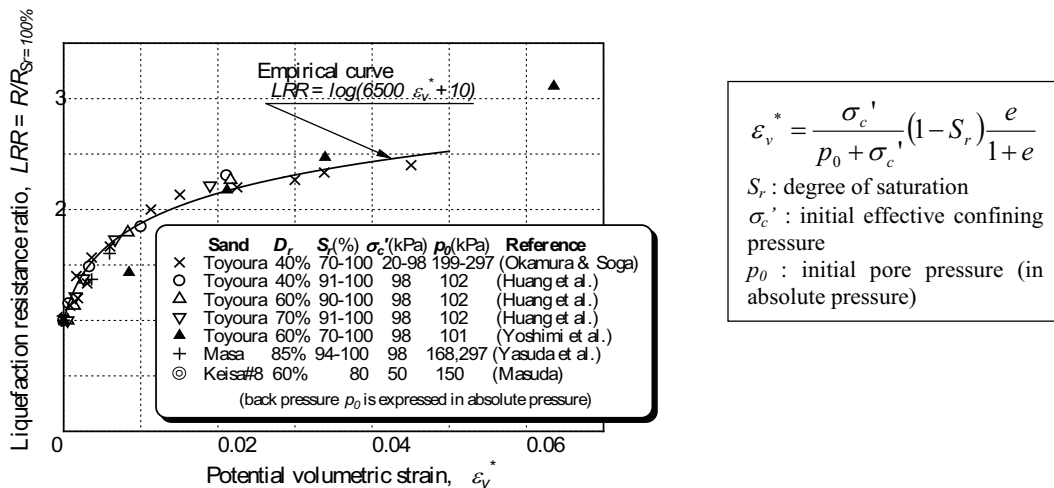p_0 : initial pore pressure (in absolute pressure)

Figure 7. Relationship between hypothetical volumetric strain and liquefaction resistance of partially saturated sand (after Okamura & Soga, 2006).

It is well recognized that unsaturated soils exhibit higher liquefaction resistance than fully saturated soils. The underlying mechanism that enhances liquefaction resistances of the unsaturated sand is such that air in a partially saturated sand absorbs generated excess pore

pressures by reducing its volume (Okamura and Soga, 2006; Unno et al., 2008). Okamura & Soga (2006) have found the unique relationship between liquefaction resistance ratios, LRR, that is the ratio of liquefaction resistance of a sand to that of fully a saturated sand, and the potential volumetric strain as shown in Figure 7 and approximated with an equation, $LRR=$ $\log(6500\varepsilon_v{}^*+10)$. The volumetric strain is caused by contraction of air in the soil according to excess pore pressure generation. The potential volumetric strain is a volumetric strain that will be attained when the excess pore pressure reaches its maximum value.

Since the drainage during shaking observed in the centrifuge tests and reducing pore volume of unsaturated soils, both result in the contraction in soil volume, may have similar effects on the liquefaction resistance, an attempt is made in this study to estimate the amount of water expelled from the saturated sand layers during shaking and resulting volumetric strains. Being a direct and promising method, measurement of surface settlement in a good accuracy was difficult especially for the thin sand layers in a centrifuge. Amount of water to be expelled during a time duration t_d from a sand layer with a thickness H with an impermeable boundary at the base is estimated as $V_d = k \cdot i \cdot t_d$. When the excess pore water pressure ratio of the sand layer reaches unity, hydraulic gradient attains its maximum value as, $i_{max} = \sigma_v{}'/\gamma_w H$. The volumetric strain due to the drainage can be expressed as,

$$\varepsilon_{v\,max} = \frac{k\sigma_v{}'}{\gamma_w H^2} t_d \tag{1}$$

where $\sigma_v{}'$ and γ_w denotes the effective overburden pressure at the middle height of the liquefied layer and the unit weight of water, respectively. In this calculation, t_d is assumed as the time duration from the beginning of the significant acceleration cycle till the sand liquefied.

The factors $1/F_L$ of the centrifuge models are plotted against the volumetric strain in Figure 8 together with the empirical relationship obtained from the cyclic triaxial tests on unsaturated sands. The centrifuge test results lay almost on a unique curve regardless of the overburden pressures and the relative density. The empirical equation of $LRR= \log(65000\varepsilon_v{}^*+10)$ rather than $LRR= \log(6500\varepsilon_v{}^*+10)$ provides more reasonable approximation to the centrifuge test data. The effect of drainage on the apparent liquefaction resistance can be taken into account in the liquefaction assessment by multiplying the undrained liquefaction resistance by $1/F_L$.

In model 2, the liquefied sand layers were overlain by unsaturated sand layers with a lower permeability due to the lower degree of saturation, drainage at the surface of the liquefied layers might be impeded. In Figure 8, however, there are no distinct differences in F_L value between model 1 and 2. In a saturated sand layer with the overburden pressures, the hydraulic gradient will be significantly high at the surface of the layer, which might accelerate drainage at shallower depth. In fact, the excess pore pressure ratios at shallower location of model 2(labeled "A" in Figure 2(b)) to be lower than locations B and C at the beginning of shaking, which was unlike model 1. It can be concluded that the two effects counterbalanced each other and the equation (1) gave reasonable volumetric strain for model 2.
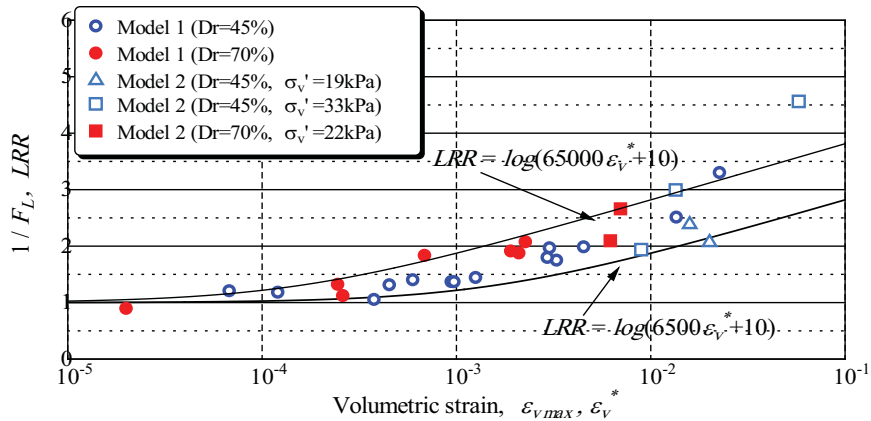
Figure 8. Relationship between rates of increase in apparent liquefaction resistance and volumetric strain due to drainage.

Conclusions

It has been reported that the current method of in-situ liquefaction potential assessment provides the factor of safety against liquefaction, F_L, for relatively thin saturated layers in levees excessively on the safe side. A possible reason for this was considered to be drainage of generated excess pore pressure during the earthquake shaking. An attempt was made to improve the liquefaction assessment method by taking the drainage effects into account.

A series of centrifuge tests on thin sand layers was conducted to investigate effects on shaking acceleration necessary to liquefy the layers of factors including relative density, permeability of sand and overburden pressure. The input acceleration necessary to cause liquefaction and thus an apparent liquefaction resistance increased with increasing permeability of the sand. Since the drainage of pore fluid is suggested to be responsible for the increase in the apparent liquefaction resistance, volume of drained fluid and the resultant volumetric strain before the sand liquefied was estimated. It was found that the apparent liquefaction resistance ratio increased uniquely with the volumetric strain due to the drainage. The effect of drainage on the apparent liquefaction resistance can be taken into account in the liquefaction assessment by multiplying the undrained liquefaction resistance by $1/F_L$.

Acknowledgments

References

Japan Road Association. Specifications for Highway Bridges, Part V, Earthquake Resistant Design. Maruzen (in Japanese). Maruzen: Japan, 2001.

Matsuo O. Seismic design of river embankments. *Tsuchi-to-kiso*, JGS, **47**(6), 9–12 (in Japanese), 1999.

Okamura M, Hayashi S. Damage to river levees by the 2011 Off the Pacific Coast Tohoku Earthquake and

prediction of liquefaction in levees. *Proc. The 4th Int. Conf. on Geotechnical Engineering for Disaster Mitigation and Rehabilitation*, 2014.

Okamura M, Soga Y. Effect on liquefaction resistance of volumetric strain of pore fluid, *Soils and Foundation*; **46**(5), 703-708, 2006.

River Front Center. Personal Communication, 1999.

River Bureau, Ministry of Land, Infrastructure and Transport. /http://www6.river.go.jp/riverhp_viewer/entry/y2011eb4071ffc52db6d40a124e92f499b12b83125342f.htmlS. 2011.

Sasaki Y, Tamura K, Yamamoto M, Ohbayashi J. Soil improvement work for river embankment damage by 1993 Kushirooki earthquake. *Proc. the First International Conference on Earthquake Geotechnical Engineering*; **1**: 43–48, 1995.

Tanaka T, Yasuda S, Naoi K. Liquefaction and post-liquefaction deformation characteristics of some silica sands under low confining pressure, Proc. the 30th JSCE Earthquake Engineering Symposium, 2009.

Tohoku Regional Development Bureau, Ministry of Land, Infrastructure and Transport. /http://www.thr.mlit.go.jp/Bumon/B00097/ K00360/Taiheiyouokijishinn/kenntoukai/110530/houkokusho.pdfS. 2011.